

Building a Magnetic Flux Model of Induction Motors and Testing on Hardware Systems Using DSP C2000

Dinh Van Nghiep, Nguyen Thi Mai Huong, Ngo Minh Duc, Nguyen Thi Thanh Nga, Nguyen Hong Quang*

Department of Automation, Thai Nguyen University of Technology, Viet Nam

*(Corresponding Author- ORCID: 0000-0002-0433-3094)

Abstract

Nowadays, three-phase AC motors, or induction motors (IMs), are widely used in industrial applications. In IM-driven systems requiring high control quality, the field-oriented control (FOC) method is often applied. In order to use the FOC control structure, it is required to identify the generated magnetic flux of the motor accurately. In this paper, the authors deal with the method of building the magnetic flux model of the IM motor. Besides, the accuracy of the model is proved experimentally using the DSP C2000 hardware system.

Keywords: IM, C2000, FOC, V/f Control, PWM.

I. INTRODUCTION

For specific applications that require operators or researchers, intervention in the control structure to customize the technology process is necessary. It is impossible with commercially available equipment. C2000 DSP with an open structure, strong computing power [1-5] and competitive price opens up the prospect of building a complete control structure for the IM motor. With the permanent magnet (PM) motor, [6-13] the magnetic flux of the motor was pre-formed because the rotor is made of permanent magnets. Therefore, it is possible to implement the FOC control structure when the angle of magnetic flux is precisely determined. The magnetic flux of the IM motor is formed when the motor is powered. This leads to determining the value of the flux of IM motors becomes more difficult than the PM motors. There are two methods to control the IM. The first one uses the V/f principle [14-16], in which the flux does not need to be accurately determined. The other uses the FOC method [6, 17-19], requiring construction of the magnetic flux model.

II. DYNAMIC MODEL

Equations for the flux of stator and rotor is shown in equation (1).

$$\begin{cases} \Psi_s = L_s \mathbf{i}_s + L_m \mathbf{i}_r \\ \Psi_r = L_m \mathbf{i}_s + L_r \mathbf{i}_r \end{cases} \quad (1)$$

In which:

$L_s = L_m + L_{\sigma s}$ and $L_r = L_m + L_{\sigma r}$. L_s is stator inductance, L_m is mutual inductance, L_s stator inductance, L_r rotor inductance, L_m mutual inductance, $L_{\sigma s}$ and $L_{\sigma r}$ are stator and rotor inductors, i_s is stator current, and i_r is rotor current. The IM

motor in this study is a squirrel-cage induction motor, so the rotor voltage is zero. Therefore, equations for the stator and rotor voltages are as follows:

$$\mathbf{u}_s = R_s \mathbf{i}_s + \frac{d\Psi_s}{dt} + j\omega_s \Psi_s \quad (2)$$

$$0 = R_r \mathbf{i}_r + \frac{d\Psi_r}{dt} + j\omega_r \Psi_r \quad (3)$$

In which $\omega_r = \omega_s - \omega$, with ω_r is the slip velocity, ω_s is the synchronous velocity, and ω is the rotor velocity.

From (1), (2) and (3), we have:

$$\begin{cases} \mathbf{u}_s = R_s \mathbf{i}_s + \frac{d\Psi_s}{dt} + j\omega_s \Psi_s \\ 0 = R_r \mathbf{i}_r + \frac{d\Psi_r}{dt} + j\omega_r \Psi_r \\ \Psi_s = L_s \mathbf{i}_s + L_m \mathbf{i}_r \\ \Psi_r = L_m \mathbf{i}_s + L_r \mathbf{i}_r \end{cases} \quad (4)$$

Eliminating the rotor current and the stator flux from (4), we obtain a set of equations describing the motor on the coordinate system dq as follows:

$$\begin{cases} \frac{di_{sd}}{dt} = -\left(\frac{1}{\sigma T_s} + \frac{1-\sigma}{\sigma T_r}\right) i_{sd} + \omega_s i_{sq} \\ \quad + \frac{1-\sigma}{\sigma T_r} \psi'_{rd} + \frac{1-\sigma}{\sigma} \omega \psi'_{rq} + \frac{1}{\sigma L_s} u_{sd} \\ \frac{di_{sq}}{dt} = -\omega_s i_{sd} - \left(\frac{1}{\sigma T_s} - \frac{1-\sigma}{\sigma T_r}\right) i_{sq} \\ \quad - \frac{1-\sigma}{\sigma} \omega \psi'_{rq} + \frac{1-\sigma}{\sigma T_r} \psi'_{rd} + \frac{1}{\sigma L_s} u_{sq} \\ \frac{d\psi'_{rd}}{dt} = \frac{1}{T_r} i_{sd} - \frac{1}{T_r} \psi'_{rd} + (\omega_s - \omega) \psi'_{rq} \\ \frac{d\psi'_{rd}}{dt} = \frac{1}{T_r} i_{sq} - (\omega_s - \omega) \psi'_{rd} - \frac{1}{T_r} \psi'_{rq} \end{cases} \quad (5)$$

Selecting the rotation system dq with q axis perpendicular to the flux generated by the rotor, we have $\psi_{rd} = 0$.

Substituting ψ_{rd} into (5), we have:

$$\frac{di_{sd}}{dt} = -\left(\frac{1}{\sigma T_s} + \frac{1-\sigma}{\sigma T_r}\right) i_{sd} + \omega_s i_{sq} + \frac{1-\sigma}{\sigma T_r} \psi'_{rd} + \frac{1}{\sigma L_s} u_{sd} \quad (6)$$

magnetic flux model is its ability to work independently. A voltage source that has a definite frequency and a specified synchronous angle is connected to the motor. Comparing the angle of the voltage source and the angle obtained from the magnetic flux model, we determine the angle error. The hardware system is shown in Figure 4.

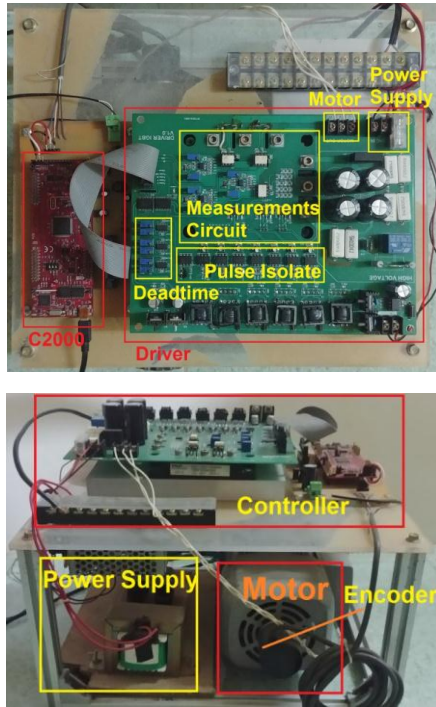


Figure 4. Controller and driver

The configuration of the supply voltage for motor testing is described in Figure 5.

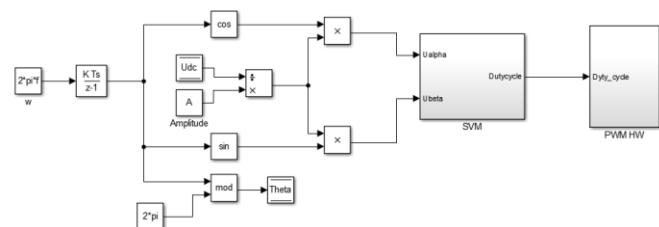


Figure 5. Motor control voltage

The collected parameters include rotor flux, synchronizing angle of the inverter, synchronous angle of the model, current I_d , I_q .

V. EXPERIMENTAL RESULTS

The whole structure of the magnetic flux model and the voltage source was designed on Matlab/Simulink software and compiled for C2000 microcontroller. The conditions and model parameters are provided in Table 1.

Table 1. Motor parameters used in experiments

Motor parameters	Symbol	Value
Rated power	P_{nom}	0.1 kW
Rated speed	n_{nom}	1407 vg/ph
Rated current	I_{nom}	0.7 A _{RMS}
Number of pairs of poles	Z_p	2
Rotor resistance	R_r	13.7 Ω
Stator resistance	R_s	21.8 Ω
Rotor inductance	L_r	0.707 H
Stator inductance	L_s	0.6716 mH
Mutual inductance	L_m	0.6313 mH
Power factor	$\cos\phi$	0.67
Coefficient of total dissipation	σ	0.1607
Moment of inertia	J	0.001 kgm ²

Experimental results are shown in Figure. 6 and Figure. 7. Figure 7 shows that the synchronizing angle of the inverter and synchronous angle of the model are almost the same. The error between the two values is the angle error of the synchronous magnetic field and the rotor flux.

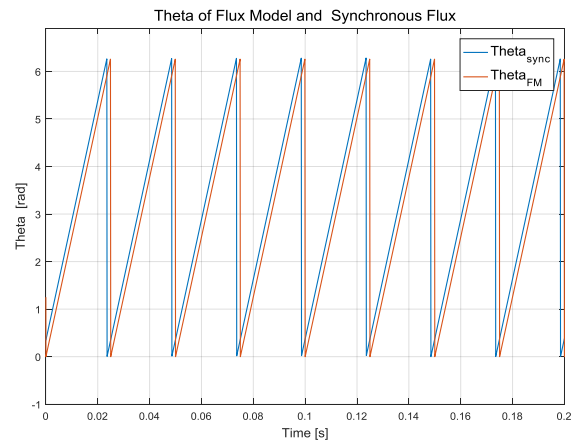


Figure 6. Experimental results of measuring the magnetic flux angle

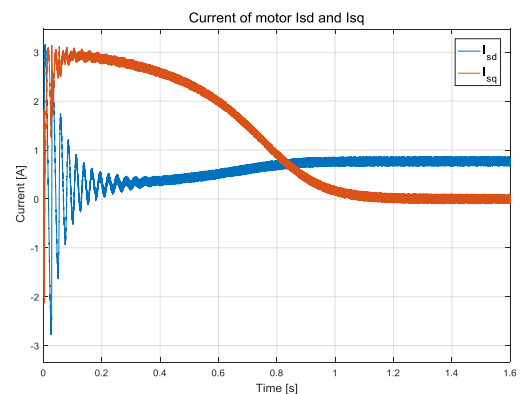


Figure 7. Experimental results of I_{dq} of the magnetic flux model

VI. CONCLUSION

Experimental results have proved the calculation ability of algorithms for magnetic flux models of three-phase asynchronous motors of C2000 series microcontrollers. The construction of an accurate magnetic flux model allows implementing the FOC control structure for the IM motor. In our future projects, the FOC control method and advanced control algorithms on hardware platforms using DSP C2000 will be implemented and installed on real systems.

REFERENCES

- [1] A. Bilal and C. Chris, 2010, "Digital motor control methodology for C2000™ Real-Time control microcontrollers, texas instruments,".
- [2] Hafizah S, Texas, 2018, "Texas instruments, TMS320F2806x Piccolo™ microcontrollers datasheet (Rev. G),".
- [3] Texas,2019, "Texas instruments, launchxl - F28069 overview,".
- [4] Texas, 2017, "Texas instruments, TMS320x2806x piccolo technical reference guide,".
- [5] Agilent, 2002, "Agilent technologies, isolation amplifier technical data,".
- [6] N. Quang and J. Dittrich, 2008, Vector control of three-phase AC machines – system development in the practice: Springer Berlin Heidelberg.
- [7] N. H. Quang et al, 2017, "Design an exact linearization controller for permanent stimulation synchronous linear motor polysolenoid," *SSRG International Journal of Electrical and Electronics Engineering*, vol. 4, pp. 7-12.
- [8] Quang. N. H et al, 2016, "Flatness Based Control Structure for Polysolenoid Permanent Stimulation Linear Motors," *SSRG International Journal of Electrical and Electronics Engineering*, vol. 3(12), pp. 31-37.
- [9] N. H. Quang et al, 2017, "Multi parametric programming based model predictive control for tracking control of polysolenoid linear motor," *Special issue on Measurement, Control and Automation*, vol. 19, pp. 31-37.
- [10] N. H. Quang et al, 2018, "Min max model predictive control for polysolenoid linear motor," *International Journal of Power Electronics and Drive Systems*, vol. 9, pp. 1666-1675.
- [11] N. H. Quang, et al, 2019, "Multi parametric model predictive control based on laguerre model for permanent magnet linear synchronous motors," *International Journal of Electrical and Computer Engineering*, vol. 9, pp. 1067-1077.
- [12] P. N. Dao et al, 2017, "Multi parametric programming and exact linearization based model predictive control of a permanent magnet linear synchronous motor," in *International Conference on System Science and Engineering*, 2017, pp. 743-747.
- [13] N. H. Quang et al, 2019, *On Tracking Control Problem for Polysolenoid Motor Model Predictive Approach*. *International Journal of Electrical and Computer Engineering (IJECE)*, vol 10, No.1, pp.849-855.
- [14] B. Ion and A. N. Syed, 2002, *The induction machine handbook*: CRC Press.
- [15] Behera, Pabitra Kumar et al. "Speed Control of Induction Motor using Scalar Control Technique." (2014)..
- [16] Texas Instruments, 2013, "Texas instruments, scalar (V/f) control of 3-phase induction motors , application report, SPRABQ8-July 2013,".
- [17] A. Bilal and B. Manish, 2013, Sensored field oriented control of 3-Phase induction motors, C2000 systems and applications: Texas Instruments, Inc.
- [18] E. K. Karrar and S. M. Ajang, 2010, "Field oriented control of induction motor," 2010.
- [19] A.-R. Haitham, I. Atif, and G. Jaroslaw, 2012, *High performance control of AC drives with MATLAB/Simulink models*: John Wiley & Sons.